

**RESEARCH ARTICLE**

Inferior vena cava revisited – Real-time flow MRI of respiratory maneuvers

Arun A. Joseph¹ | Dirk Voit¹ | Jens Frahm^{1,2}¹Biomedizinische NMR, Max-Planck-Institut für biophysikalische Chemie, Göttingen, Germany²DZHK (German Centre for Cardiovascular Research), partner site Göttingen, Germany**Correspondence**D. Voit, Biomedizinische NMR, Max-Planck-Institut für biophysikalische Chemie, 37070, Göttingen, Germany.
Email: dvoit@gwdg.de

Recent MRI studies of blood flow in the inferior vena cava (IVC) resulted in findings which are inconsistent with earlier observations by invasive procedures – most likely because ECG-gated MRI techniques are unable to resolve dynamic adjustments due to respiration. The purpose of this work was to apply real-time phase-contrast MRI at 50 ms resolution to re-evaluate IVC flow in response to normal and deep breathing as well as breath holding and Valsalva maneuver (11 young healthy subjects). Real-time flow MRI relied on highly undersampled radial gradient-echo sequences and a model-based nonlinear inverse reconstruction. A frequency analysis of the predominant pulsatility classified IVC flow in individual subjects as “cardiac”, “respiratory” or “mixed” type. Peak flow velocities during free breathing ranged from 30 to 58 cm s⁻¹, while flow rates varied from 15 to 37 ml s⁻¹. The subject-specific IVC flow pattern persists during deep breathing although the enhanced respiratory influence may shift subjects from “cardiac” to “mixed” or from “mixed” to “respiratory” type. Peak velocities increased relative to normal breathing but led to similar flow rates of 16 to 34 ml s⁻¹. Inspiration during deep breathing elicited brief periods of flow reversal in all subjects with mean peak velocities of –21 cm s⁻¹. The observation of only mildly flattened parabolic velocity distributions within the IVC indicated mostly laminar flow. Breath holding reduced blood flow velocities and rates by more than 40% on average, while Valsalva maneuvers completely abolished venous return. In conclusion, IVC blood flow is dominated by the acquired respiratory behavior of individual subjects and its pressure-induced alterations relative to cardiac pulsation. The responses to breath holding and Valsalva maneuver are in full agreement with previous invasive observations of reduced or even ceased flow, respectively.

KEYWORDS

inferior vena cava, phase-contrast flow MRI, real-time MRI

1 | INTRODUCTION

In a 1968 seminal paper Wexler et al¹ for the first time studied caval blood flow in conscious human subjects using a catheter-tip electromagnetic transducer. The measurements were restricted to flow velocity as changes of the inferior vena cava (IVC) lumen could not be assessed, but

List of Abbreviations: ECG, Electrocardiogram; IVC, Inferior vena cava; VENC, Encoding velocity.

This is an open access article under the terms of the Creative Commons Attribution-NonCommercial-NoDerivs License, which permits use and distribution in any medium, provided the original work is properly cited, the use is non-commercial and no modifications or adaptations are made.

© 2020 The Authors. NMR in Biomedicine published by John Wiley & Sons Ltd

provided guiding insights into the responses of venous return to a variety of respiratory conditions including normal and deep breathing as well as Valsalva maneuver. In particular, the study served to establish the IVC as a collapsible vessel which is subject to respiratory pressure and, for example, during deep inspiration (i.e., low intrathoracic pressure) collapses near the diaphragm and paradoxically reduces the venous return to the heart.²

More detailed quantitative physiologic data of IVC flow were attempted by Cheng et al³ in a first ECG-synchronized phase-contrast flow MRI study. These CINE MRI techniques measure through-plane flow velocities by taking the phase difference of two images with different velocity-encoding (VENC) gradients. However, the data from multiple heartbeats are retrospectively sorted according to the cardiac cycle, so that the approach implicitly assumes (cardiac) periodicity. The authors reported infrarenal IVC flow rates of $20 \pm 8 \text{ ml s}^{-1}$ during rest and $88 \pm 15 \text{ ml s}^{-1}$ during exercise (11 young subjects), but admitted that CINE MRI techniques can only deliver time-averaged values over multiple heartbeats without resolving any respiratory dynamics. In a different study using the same CINE flow MRI technique related methodologic complications may have affected the unexpected observation of high IVC flow rates of about 60 ml per heartbeat during breath holding and Valsalva maneuver,⁴ whereas previous invasive work documented close to zero velocity under similar conditions.¹

In order to resolve the aforementioned ambiguities with CINE flow MRI this study revisits IVC flow with use of a novel MRI method which offers true real-time flow measurements at high temporal and spatial resolution. The approach is based on the extension of anatomic real-time MRI⁵ to real-time flow MRI⁶ which together enable hitherto impossible developments and applications.⁷ Technically, the concept combines highly undersampled radial gradient-echo sequences and regularized nonlinear inverse reconstructions. Real-time flow MRI therefore allows for an unbiased dynamic assessment of IVC flow independent of any cardiac periodicity and in full response to respiration-induced variations. Here, we study IVC flow in normal subjects at 50 ms temporal resolution during normal and deep breathing as well as in response to breath holding and Valsalva maneuver.

2 | METHODS

All MRI measurements were performed at 3 T (Magnetom Prisma fit, Siemens Healthineers, Erlangen, Germany) with use of an 18-element thorax coil in conjunction with suitable elements of the spine coil array. Eleven subjects (8 male, 3 female, mean age 28 ± 8 years, range 19–45 years) without known illness participated in the study. Written informed consent, according to the recommendations of the local ethics committee, was obtained from all subjects prior to MRI.

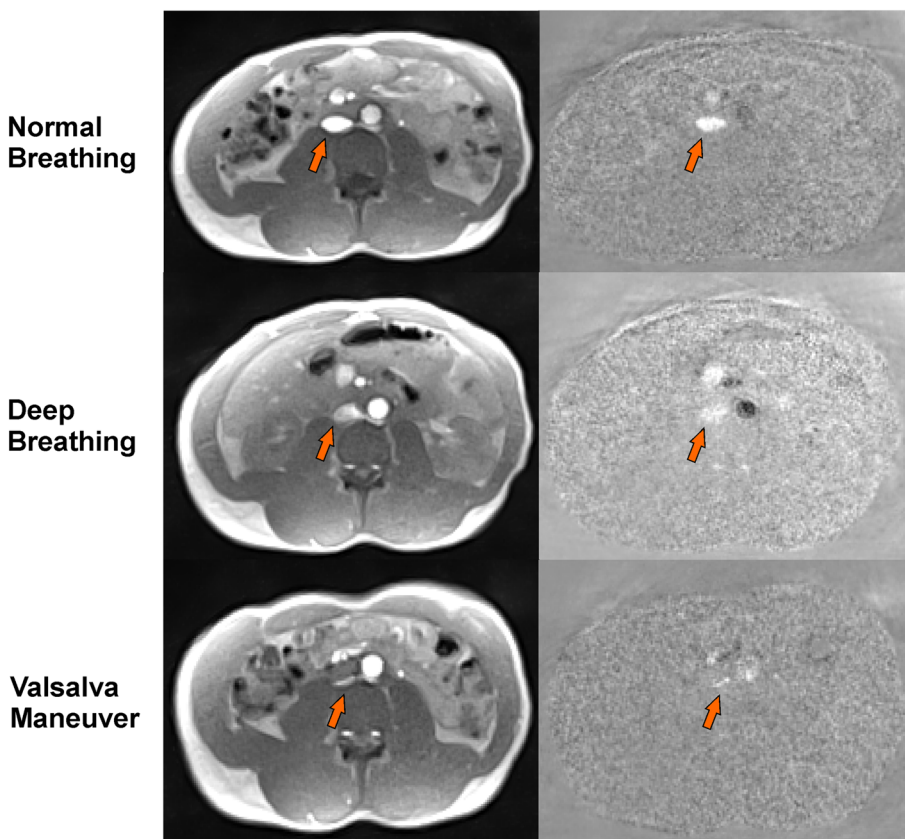


FIGURE 1 Real-time flow MRI of the infrarenal IVC (arrows) at inspiration (normal and deep breathing) and during Valsalva maneuver. (left) anatomic images and (right) corresponding phase-contrast velocity maps of subject #7 (table 1) selected from real-time flow MRI movies at 50 ms temporal and $1.5 \times 1.5 \times 6.0 \text{ mm}^3$ spatial resolution

All subjects underwent real-time flow MRI of the IVC at 50 ms resolution during the performance of different respiratory protocols: (1) normal (free) breathing for 30 s (600 frames, i.e. pairs of anatomic images and phase-contrast velocity maps), (2) deep breathing comprising 5 s of normal breathing, 20 s of deep breathing and 20 s of normal breathing (900 frames), (3) breath holding comprising 5 s of normal breathing, 10 s of breath holding (with either inspiration or exhalation) and 20 s of normal breathing (700 frames), and (4) Valsalva maneuver comprising 5 s of normal breathing, 10 s of Valsalva maneuver and 20 s of normal breathing (700 frames). Flow parameters were assessed in transverse sections (field of view 384 mm) perpendicular to the infrarenal portion of the IVC about midway between the renal veins and the iliac bifurcation at an in-plane resolution of $1.5 \times 1.5 \text{ mm}^2$ and 6 mm slice thickness. This position is usually chosen for the implantation of medical devices, so that respective flow

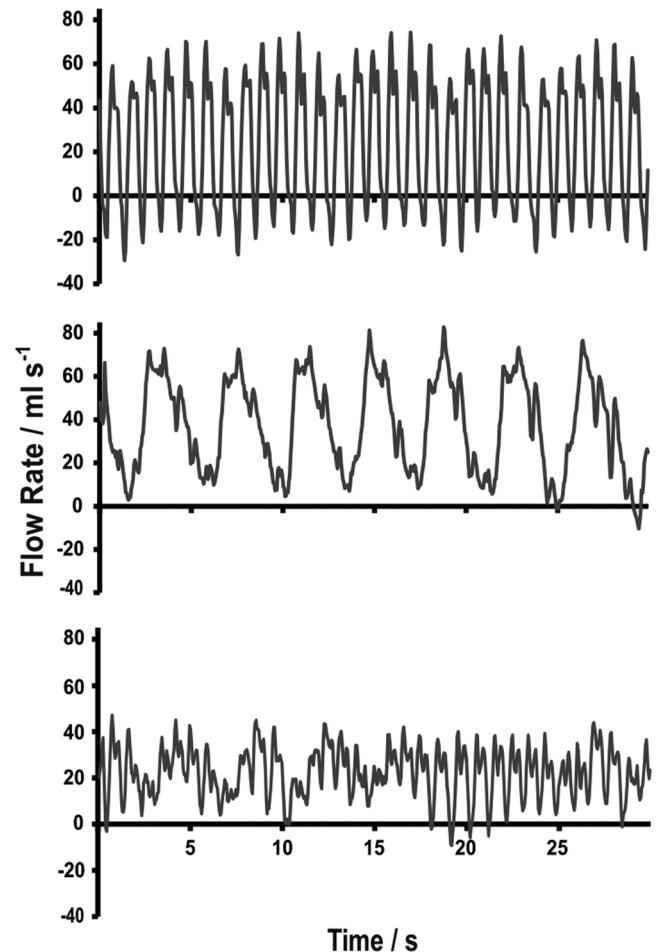


FIGURE 2 Real-time flow MRI of the IVC during free breathing. Time courses of mean flow rates (ml s^{-1}) for a 30 s protocol (600 frames) and three representative subjects with a (top) “cardiac”, (middle) “respiratory”, and (bottom) former “mixed” now “respiratory” temporal pattern (subjects #3, #7 and #10 in table 1, respectively)

TABLE 1 Real-time flow MRI of the infrarenal IVC: Frequency analysis

Subject	Normal breathing			Deep breathing		
	Power 0–0.5 Hz	Power 0.6–2.0 Hz	Category	Power 0–0.5 Hz	Power 0.6–2.0 Hz	Category
#1	18	25	Mixed	18	6.1	Respiratory
#2	14	9.9	Mixed	23	3.5	Respiratory
#3	4.8	21	Cardiac	4.1	17	Cardiac
#4	6.7	5.5	Mixed	5.3	3.7	Mixed
#5	4.8	30	Cardiac	4.1	22	Cardiac
#6	7.1	2.3	Respiratory	12	2.7	Respiratory
#7	23	3.2	Respiratory	24	2.9	Respiratory
#8	13	2.8	Respiratory	5.8	2.1	Respiratory
#9	5.4	23	Cardiac	18	11	Mixed
#10	5.2	5.8	Mixed	14	2.7	Respiratory
#11	4.4	24	Cardiac	13	8.5	Mixed

patterns are of particular interest. A typical example is the permanent or temporary placement of an IVC filter which serves to avoid pulmonary embolism by precluding the upward movement of a thrombus from peripheral veins.

Through-plane phase-contrast flow MRI in real time is accomplished by acquiring series of two high-speed real-time MRI datasets with different flow-encoding gradients.⁶ Relevant acquisition parameters are: repetition time 2.78 ms, echo time 2.11 ms (30% asymmetry), flip angle 10° with randomized radiofrequency phases,⁸ and through-plane flow-encoding gradients with VENC 120 cm s⁻¹. Moreover, the automatic acquisition of a few body coil images during the prep scan period serves to initialize the iterative numerical reconstruction from multi-coil data in order to exclude the eventual occurrence of phase singularities that lead to “black holes” in magnitude images.⁹ The use of only 9 radial spokes per flow-encoding dataset results in a total acquisition time of $2 \times 9 \times 2.78$ ms = 50.04 ms for one frame, i.e. a pair of anatomic image and corresponding velocity map. These optimized choices represent a compromise between the needs for a large field of view, adequate spatial and temporal resolution, and reliable reconstructions in terms of image quality and velocity quantitation.

The algorithm for serial image reconstruction takes advantage of an advanced model-based approach with automatic scaling^{10,11} that jointly computes an anatomic image, all coil sensitivity maps and a phase-contrast velocity map directly from the raw data – rather than relying on a

TABLE 2 Real-time flow MRI of the infrarenal IVC: Velocities and flow rates

Respiration	Peak velocity* Cm s ⁻¹	Mean velocity† Cm s ⁻¹	Flow rate‡ ml s ⁻¹
Normal breathing	36.6 ± 9.1 (30–58)	7.7 ± 3.1 (4.4–14.8)	23.6 ± 5.4 (15–37)
Deep breathing	45.6 ± 14.3 (31–83)	7.5 ± 3.1 (4.8–15.8)	22.7 ± 5.7 (16–34)
Breath holding	25.8 ± 11.2 (9–29)	4.4 ± 2.7 (0.3–6.6)	13.3 ± 7.1 (2–20)
Valsalva	-	0.2 ± 1.4	0.2 ± 1.9

Values represent mean ± standard deviation averaged across subjects ($n = 11$), while brackets indicate range.

*Single-pixel peak value during maneuver.

†Mean across the IVC lumen and duration of maneuver.

‡Mean across duration of maneuver.

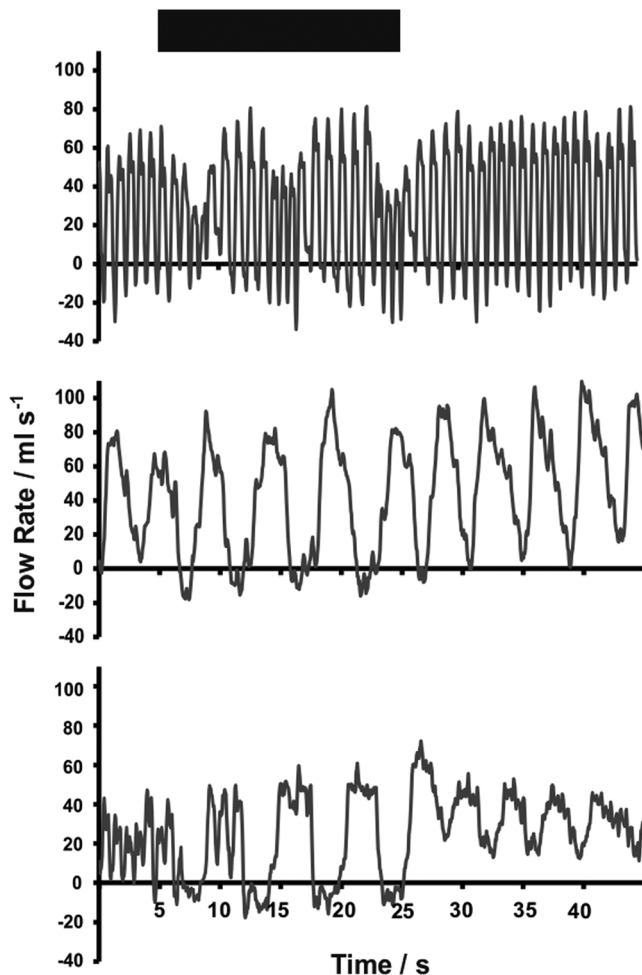


FIGURE 3 Real-time flow MRI of the IVC during deep breathing. Time courses of mean flow rates (ml s⁻¹) for a 45 s protocol (900 frames) comprising 5 s of normal breathing, 20 s of deep breathing (black bar) and 20 s of normal breathing (same subjects as for Figure 2)

complex subtraction of two separately calculated images with different flow-related phase information. As previously demonstrated this method improves the spatiotemporal resolution and yields velocity maps without “salt-and-pepper” noise in image regions without signal support.¹⁰ Corrections of background phase which are typical for flow MRI techniques based on complex subtraction are not required for model-based reconstructions which iteratively estimate phase-contrast maps with initialization by zero velocity. Moreover, for the present conditions (i.e., relatively high velocities, IVC at isocenter) concomitant gradient fields are not considered, but need to be corrected for low velocities and off-center measurements. As a post-processing step spatial denoising with a modified local means filter¹² and temporal median filtering is only applied to anatomic images, but not to velocity maps to preserve temporal fidelity.¹³ Figure 1 demonstrates the resulting quality by selected anatomic images and corresponding velocity maps taken from real-time flow MRI movies obtained during normal and deep breathing as well as during Valsalva maneuver.

Online reconstruction and display of real-time images is achieved by a highly parallelized version of the reconstruction algorithm and its implementation on a computer (Sysgen, Bremen, Germany) with 8 graphical processing units (GeForce GTX, TITAN, NVIDIA, Santa Clara, CA) which is fully integrated into the reconstruction pipeline of the commercial MRI system. As a result, reconstruction and online visualization of serial anatomic images and velocity maps begin immediately after starting the measurement (i.e., data acquisition) and continue during scanning with a slightly increasing lag time which depends on the matrix resolution.

Analysis of real-time flow MRI data, in particular a fully automatic segmentation of the IVC, is performed with use of the prototype software CaFuR¹⁴ (Fraunhofer Mevis, Bremen, Germany, Version 1.1). These newly developed algorithms are capable to process large datasets which in this study reach 900 frames per protocol. For all breathing maneuvers the analyses include a determination of single-pixel peak flow velocities that occur during the performance of a specific breathing condition. However, more reliable metrics which better represent the true flow refer to mean velocities averaged across the vessel lumen as well as the time-averaged mean flow rates derived therefrom. Respective values are given as mean values (\pm standard deviation) averaged across subjects. Frequency analyses of temporal flow responses were done in MATLAB (MathWorks, Natick, MA). The pulsatility pattern of IVC flow during normal and deep breathing was assessed by computing the power (i.e., the magnitude of the Fourier transform of respective time courses) of respiratory-related frequencies (0–0.5 Hz) and cardiac-related frequencies (0.6–2.0 Hz).

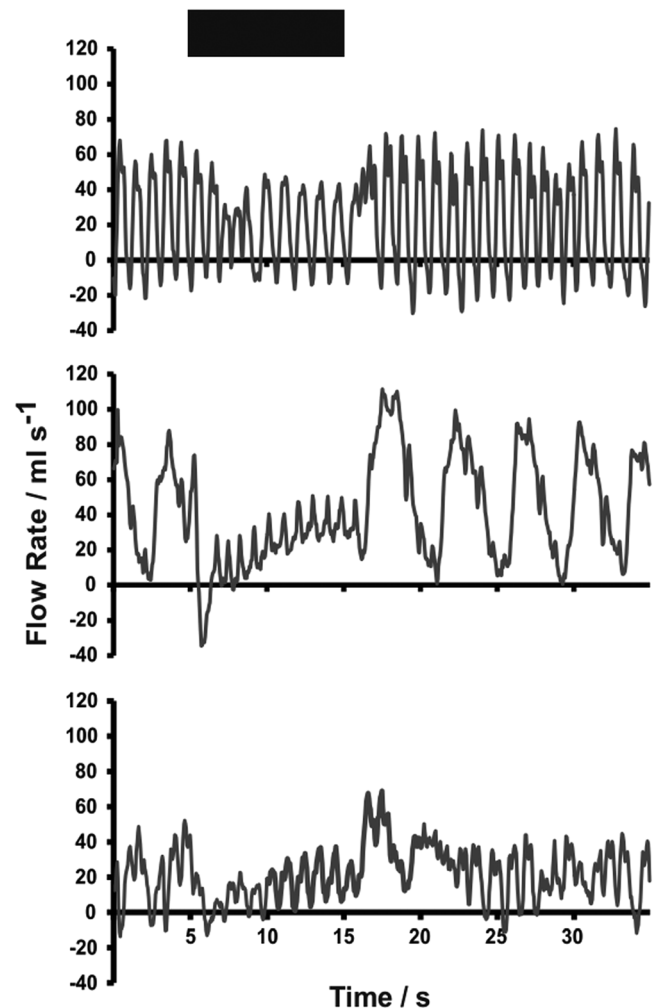


FIGURE 4 Real-time flow MRI of the IVC during breath holding. Time courses of mean flow rates (ml s^{-1}) for a 35 s protocol (700 frames) comprising 5 s of normal breathing, 10 s of breath holding with inspiration (black bar) and 20 s of normal breathing (same subjects as for Figure 2)

3 | RESULTS

Under normal breathing conditions venous return in the infrarenal IVC presents with different temporal patterns in individual subjects. However, the observed profiles may be grouped into three categories as qualitatively demonstrated in Figure 2 which shows time courses of IVC flow rates for a 30 s period of normal (free) breathing in three representative subjects. The predominance of a high-frequency response pattern (Figure 2, top) relates to a “cardiac” type where the pulsatility is determined by the periodicity of the cardiac cycle. This temporal flow profile is superimposed by only a mild modulation due to respiration which in this case corresponds to a 6 s breathing cycle (i.e., 120 frames). In contrast, the temporal pattern for subjects of the “respiratory” type (Figure 2, middle) is dominated by the breathing cycle (here about 4 s or 80 frames) and superimposed with minor variations due to cardiac pulsatility (see also Suppl. Video S1). Finally, a third group of subjects may be characterized as “mixed” type (Figure 2, bottom) with variable contributions of both cardiac and respiratory-induced flow changes. These observations are quantitatively confirmed by a frequency analysis of the temporal flow profiles. The three types mentioned above are characterized by the power of the ranges for respiratory-related (0–0.5 Hz) and cardiac-related frequencies (0.6–2.0 Hz). Respective results are given in Table 1 for all subjects under normal and deep breathing conditions. Quantitative results for peak and mean flow velocities as well as mean flow rates per respiratory condition are summarized in Table 2 merging data for all three IVC flow types.

It turns out that the basic IVC flow characteristics are largely persistent within subjects although a stronger respiratory influence may shift subjects from “cardiac” to “mixed” or from “mixed” to “respiratory” type (e.g., see subjects #9 and #10 in Table 1, respectively). This intrasubject stability most likely reflects an established respiratory behavior which leads to the preservation of principle pulsatility features despite modulations by breathing maneuvers. For example, Figure 3 depicts the responses to deep breathing for the same subjects studied in Figure 2. For the “cardiac” and “mixed” type the respiratory modulation becomes more pronounced so that the “mixed” type moves into the “respiratory” category (subject #10 in Table 1). The “respiratory” type reveals higher flow rates and shorter breathing cycles in line with the actual performance (see also Suppl. Video S2). In terms of quantitative values (Table 2), the peak velocity increases by about 25% to 45.6 cm s^{-1} , but the mean flow rate remains unchanged. Another finding, which extends eventual observations during normal breathing, is the occurrence of brief periods of flow reversal during deep inspiration, i.e. low intrathoracic pressure, for all subjects. The temporal assignment is confirmed by the simultaneously

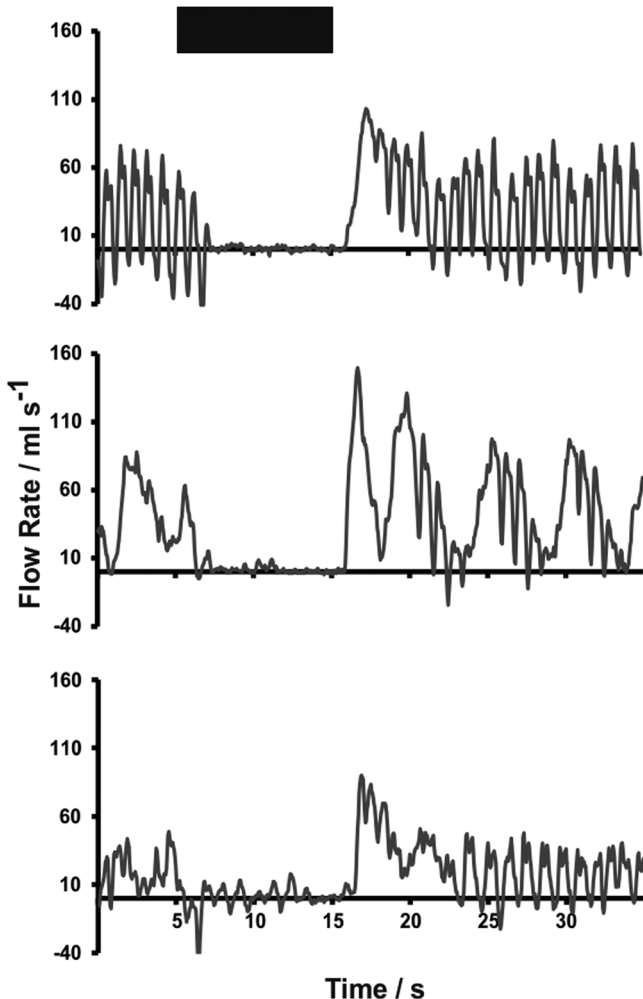


FIGURE 5 Real-time flow MRI of the IVC during Valsalva maneuver. Time courses of mean flow rates (ml s^{-1}) for a 35 s protocol (700 images) comprising 5 s of normal breathing, 10 s of Valsalva maneuver (black bar) and 20 s of normal breathing (same subjects as for Figure 2)

recorded anatomic real-time images (i.e., transverse sections as in Figure 1) which clearly delineate movements of the abdominal wall in response to breathing (see Suppl. Video S2 for the “respiratory” type with deep breathing). Quantitatively, the reverse IVC flow presents with mean peak velocities of -15 cm s^{-1} for normal breathing and -21 cm s^{-1} for deep breathing.

Figures 4 and 5 refer to the IVC flow profiles in response to protocols with breath holding and Valsalva maneuver, respectively. The traces again refer to the same subjects as in Figures 2 and 3, while the corresponding Suppl. Videos S3 and S4 present the corresponding real-time flow MRI movies during breath holding and Valsalva maneuver of subject #7 (middle panel). Qualitatively, the breath-holding profile for the “respiratory” type (Figure 4, middle) clearly demonstrates the predominance of cardiac pulsation in the absence of breathing and thus demonstrates mutual independence and superposition of both contributions. In quantitative terms, breath holding – regardless of inspiration or exhalation (data not shown) – reduces blood flow in the IVC to a variable degree in individual subjects most likely depending on actual performance. The mean flow rate of 13.3 ml s^{-1} is reduced by more than 40% relative to normal or deep breathing (Table 2). On the other hand, a Valsalva maneuver generates a high intraabdominal pressure sufficient to completely abolish venous return in all cases. This is quantitatively confirmed (Table 2) with mean velocities and flow rates close to zero. In all cases, release of the Valsalva maneuver is followed by an immediate and strong respiratory-induced increase of IVC flow (Figure 5) before subjects recover their individual flow pattern.

Finally, Figure 6 depicts velocity distributions within the IVC during both normal and deep breathing as well as at peak forward flow and peak backward flow (for the complete 45 s movie representation with 20 s of deep breathing see Suppl. Video S5). The color-coded maps originate from fixed rectangular regions-of-interest of 2 to 3 cm length selecting the vessel only. The data demonstrate that flow within the IVC of normal subjects at rest presents with an only mildly flattened parabolic velocity distribution which hints to the predominance of laminar flow characteristics.

4 | DISCUSSION

This work exploits a novel real-time flow MRI technique to revisit blood flow in the infrarenal IVC and its dynamic responses to respiratory maneuvers in an unbiased manner. A main finding is the observation that IVC blood flow is largely dominated by the respiratory behavior acquired

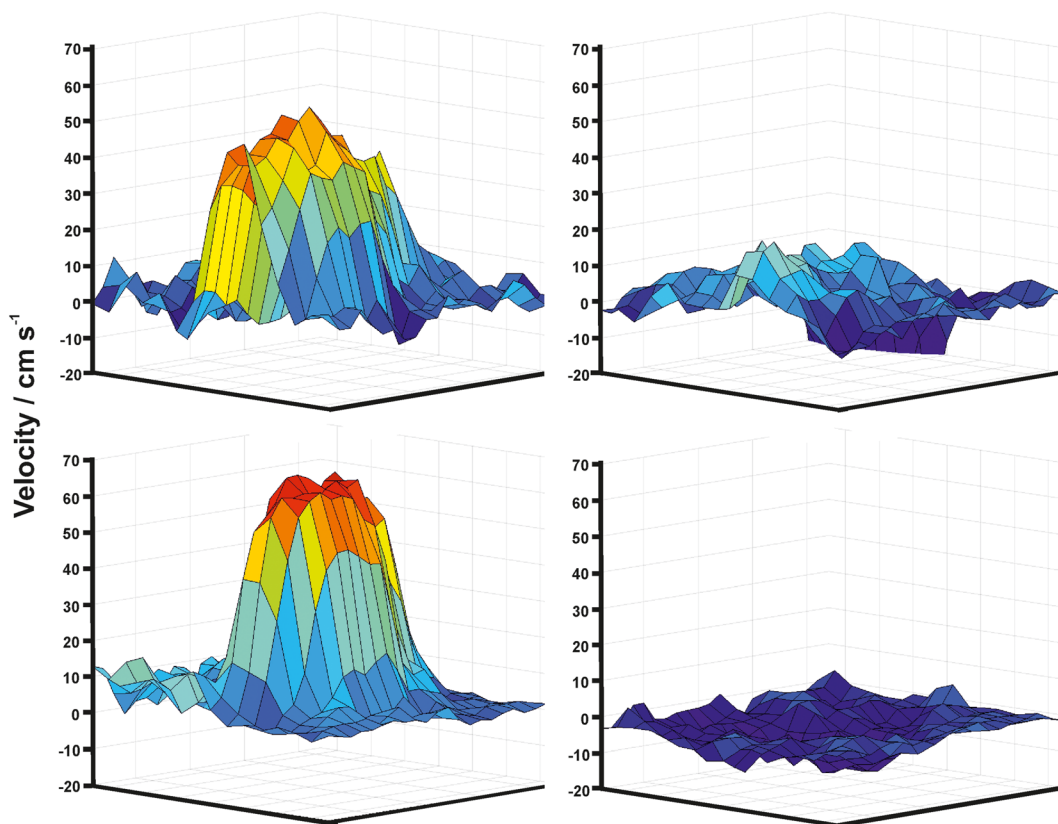


FIGURE 6 Velocity profiles within the IVC during normal and deep breathing. Color-coded maps representing the distribution of blood flow velocities (cm s^{-1}) within the IVC at (left) peak forward flow and (right) peak backward flow during (top) normal and (bottom) deep breathing (subject #7 as in middle panel of Figure 2)

by individual subjects. Accordingly, the temporal flow patterns may be grossly grouped into a “cardiac”, “respiratory” and “mixed” category where the pulsatile nature is either dominated by cardiac periodicity or respiratory cycling or a mixture of both. In general, both pressure-mediated contributions are independent of each other, so that respective flow effects superimpose. It seems plausible that weak thoracic breathers are likely to constitute the “cardiac” type, whereas strong abdominal breathers belong to the “respiratory” group, although other contributions cannot be excluded.

A second main finding is the fact that the specific responses to breath holding and Valsalva maneuver, i.e. the respective dynamic adjustments of IVC flow velocities and rates, are in excellent agreement with previous invasive observations¹ of decreased or even ceased flow, respectively. The same holds true for quantitative peak flow velocities of about 35 to 45 cm s⁻¹ during normal and deep breathing,¹ while flow rates of about 23 ml s⁻¹ match values obtained by ECG-gated flow MRI.³ The similarity of mean flow velocities and rates for normal and deep breathing (Table 1) suggests that free breathing is effective enough to ensure complete venous return – at least in a group of young healthy subjects and in a resting state. This is paralleled by the observation of a nearly laminar flow pattern under such circumstances.

A major limitation of this study is the small cohort of subjects and the lack of patient studies. In particular, putative alterations of IVC flow characteristics due to physical exercise or in patients with compromised breathing performance remain to be investigated. A further (though transient) restriction is limited access to the chosen methodology which is not yet commercially available.

In conclusion, real-time flow MRI of the IVC in normal subjects overcomes ambiguities of ECG-gated CINE flow MRI studies which are unable to resolve respiratory dynamics. The finding of inter-individual variability but intrasubject stability of temporal IVC flow profiles suggests the need to monitor flow characteristics in each individual subject both for diagnostic studies or the planning of therapeutic interventions. This particularly applies to candidates for the implantation of medical devices in the IVC.

ORCID

Dirk Voit  <https://orcid.org/0000-0002-0058-2157>

REFERENCES

1. Wexler L, Bergel DH, Gabe IT, Makin GS, Mill CJ. Velocity of blood flow in normal human venae cavae. *Circ Res.* 1968;23:349-359.
2. Gardner AMN, Turner MJ, Wilmshurst CC, Griffiths DJ. Hydrodynamics of blood through the inferior vena cava. *Med Biol Eng Comput.* 1977;15:248-253.
3. Cheng CP, Herfkens RJ, Taylor CA. Inferior vena cava hemodynamics quantified in vivo at rest and during cycling exercise using magnetic resonance imaging. *Am J Physiol Heart Circ Physiol.* 2003;284:H1161-H1167.
4. Kuzo RS, Pooley RA, Crook JE, Heckman MG, Gerber TC. Measurement of caval flow with MRI during respiratory maneuvers: implications for vascular contrast opacification on pulmonary CT angiographic studies. *Am J Radiol.* 2007;188:839-842.
5. Uecker M, Zhang S, Voit D, Karaus A, Merboldt KD, Frahm J. Real-time MRI at a resolution of 20 ms. *NMR Biomed.* 2010;23:986-994.
6. Untenberger M, Tan Z, Voit D, et al. Advances in real-time phase-contrast flow MRI using asymmetric radial gradient echoes. *Magn Reson Med.* 2016;75:1901-1908.
7. Frahm J, Voit D, Uecker M. Real-time MRI – Radial gradient-echo sequences with nonlinear inverse reconstruction. *Invest Radiol.* 2019;54(12):757-766. in press
8. Roeloffs VB, Voit D, Frahm J. Spoiling without additional gradients – radial FLASH MRI with randomized radiofrequency phases. *Magn Reson Med.* 2016;75:2094-2099.
9. Voit D, Kalentev O, Frahm J. Body coil reference for inverse reconstructions of multi-coil data – The case for real-time MRI. *Quant Imaging Med Surg.* 2019;9(11):1815-1819. in press
10. Tan Z, Roeloffs VB, Voit D, et al. Model-based reconstruction for real-time phase-contrast flow MRI – improved spatiotemporal accuracy. *Magn Reson Med.* 2017;77:1082-1093.
11. Tan Z, Hohage T, Joseph AA, Wang X, Merboldt KD, Frahm J. An eigenvalue approach for the automatic scaling of unknowns in model-based reconstructions: application to real-time phase-contrast flow MRI. *NMR Biomed.* 2017;30:e3835. <https://doi.org/10.1002/nbm.3835>
12. Klosowski J, Frahm J. Image denoising for real-time MRI. *Magn Reson Med.* 2017;77:1340-1352.
13. Frahm J, Schätz S, Untenberger M, et al. On the temporal fidelity of nonlinear inverse reconstructions for real-time MRI – the motion challenge. *Open Med Imaging J.* 2014;8:1-7.
14. Zoehrer F, Huellebrand M, Chitiboi T, et al. Real-time myocardium segmentation for the assessment of cardiac function variation. In: Krol A, Gimi B, eds. *Medical Imaging 2017: Biomedical Applications in Molecular, Structural, and Functional Imaging* (pp. 101370L-1-101370L-7). Bellingham, Wash.: SPIE; 2017. <https://doi.org/10.1117/12.2254373>

SUPPORTING INFORMATION

Additional supporting information may be found online in the Supporting Information section at the end of this article.

How to cite this article: Joseph AA, Voit D, Frahm J. Inferior vena cava revisited – Real-time flow MRI of respiratory maneuvers. *NMR in Biomedicine.* 2020;e4232. <https://doi.org/10.1002/nbm.4232>